[A25] Study of Fluorescence Diffuse Optical Tomography

Mechanical Engineering and Intelligent System Department
Yamada Laboratory
0434074
Andhi Marjono

1. Introduction

There has been rapid development of optical tomography to detect the diseases origin that mostly can be found at the molecular level [1]. New optical imaging combining fluorescence and diffuse optical tomography (DOT) is emerging. Fluorescence is light emission from fluorophore when excited by light with a particular wavelength. Localized concentration of fluorophore introduced into living tissue is known to reflect the existence or growth of tumors.

We combine the fluorescence approach with the diffuse optical tomography (DOT) that will be more useful in the field of the molecular imaging. In the fluorescence DOT, by measuring the emission light distribution on the tissue surface, we can get some information on locations and concentrations of fluorophores.

In order to determine the distributions of fluorophores and internal optical properties of tissue, an accurate model of emission light propagation is essential. In this work, we develop a method to solve the photon diffusion equation for emission light using a convolution between the solutions for zero lifetime and an exponential function for a finite lifetime.

2. Mathematical Model

Assuming the optical properties of the tissue at excitation and emission wavelength are equal, propagation of emission light for zero lifetime in a scattering-absorbing medium can be described by the diffusion equations [2, 3]

$$\left[-D(\mathrm{r})\nabla^2 + \mu_a(\mathrm{r}) + \varepsilon N(\mathrm{r}) + \frac{1}{c}\frac{\partial}{\partial t}\right]\Phi_s(\mathrm{r},t) = q_s \qquad (1)$$

$$\left[-D(r)\nabla^2 + \mu_a(r) + \frac{1}{c}\frac{\partial}{\partial t}\right]\underbrace{\left(\frac{1}{\gamma}\Phi_m^*(r,t) + \Phi_s(r,t)\right)}_{\Phi_t(r,t)} = q_s \qquad (2)$$

$$\Phi_m^*(r,t) = \gamma\left(\Phi_t(r,t) - \Phi_s(r,t)\right) \qquad (3)$$

where Φ_s and Φ^*_m are the diffuse photon fluence rates for excitation and emission lights for zero lifetime (watt mm^{-2}), q_s is the excitation light source (watt mm^{-3}), c is the speed of light (0.225 mm/ps), γ is the quantum yield, D is the optical diffusion coefficients of light (mm), $N(r)$ is the spatially varying concentration, ε is the molar extinction coefficient of the fluorophore and μ_a is the absorption coefficients of the medium. The solution of the emission light including a finite lifetime of fluorescence is obtained by convolving Eq.(3) with an exponential function for fluorescence lifetime as expressed in Eq. (4) [4]

$$\Phi_m = \Phi_m^* \otimes \frac{1}{\tau} e^{-\frac{t}{\tau}} \tag{4}$$

where t is time (ps) and τ is a fluorescence lifetime (ns) and $\otimes$ indicates convolution process. We use the Robin boundary conditions at the surface of the medium given by Eq. (5)

$$-D(r)\nabla\Phi(r,t) = \frac{1}{2A}\Phi(r,t) \tag{5}$$

where A describes the internal reflection due to the refractive index mismatch between air and tissue.

3. Simulation Results and Discussion

The 2-D geometry of the problem is illustrated in Fig. 1. We use a model of circular domain (diameter R = 20 mm) with considering the potential applications to small animals. There are 3 different shapes of targets inside the model, 2 ellipses and 1 circle. An ultra-short pulse laser is incident at the top of the tissue model.

Light intensities measured at the surface are generated by solving Eq. (1) using the finite element method. The positions of three targets, source and detectors are shown in Fig. 1. The values of the optical parameters of the background and embedded object are listed in Table 1. We assume the quantum yield γ and the fluorophore lifetime τ as 0.016 and 0.56 ns, respectively.

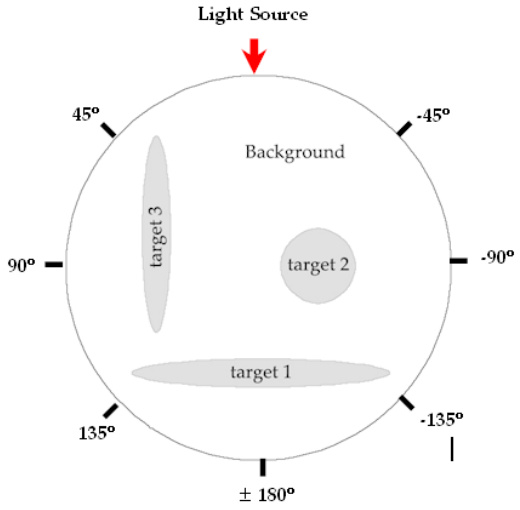

Fig. 1. Circular model with 3 embedded targets inside.

Table 1. Optical properties of the background and targets

Object	μ_a (mm^{-1})	D (mm)	Fluorophore Concentration N (μM)
Background	0.015	0.20	0.0
Targets 1,2 and 3	0.021	0.33	1.0

We show the results of 3 main detectors at the surface that are located on the left (90°), bottom (±180°) and right (-90°) side of the model. Figure 2(d) shows the distribution of light intensities measured by these detectors. The maximum value occurs at the left sensor, the nearest sensor from the target 3. Target 3 is the nearest target from the light source when illuminated on the top side of the object. It absorbs the exciting light more than others and emits it immediately to other areas. We also calculated the intensities of the emission light in case of only one target is embedded inside the model as illustrated in Fig. 2(a), 2(b) and 2(c).

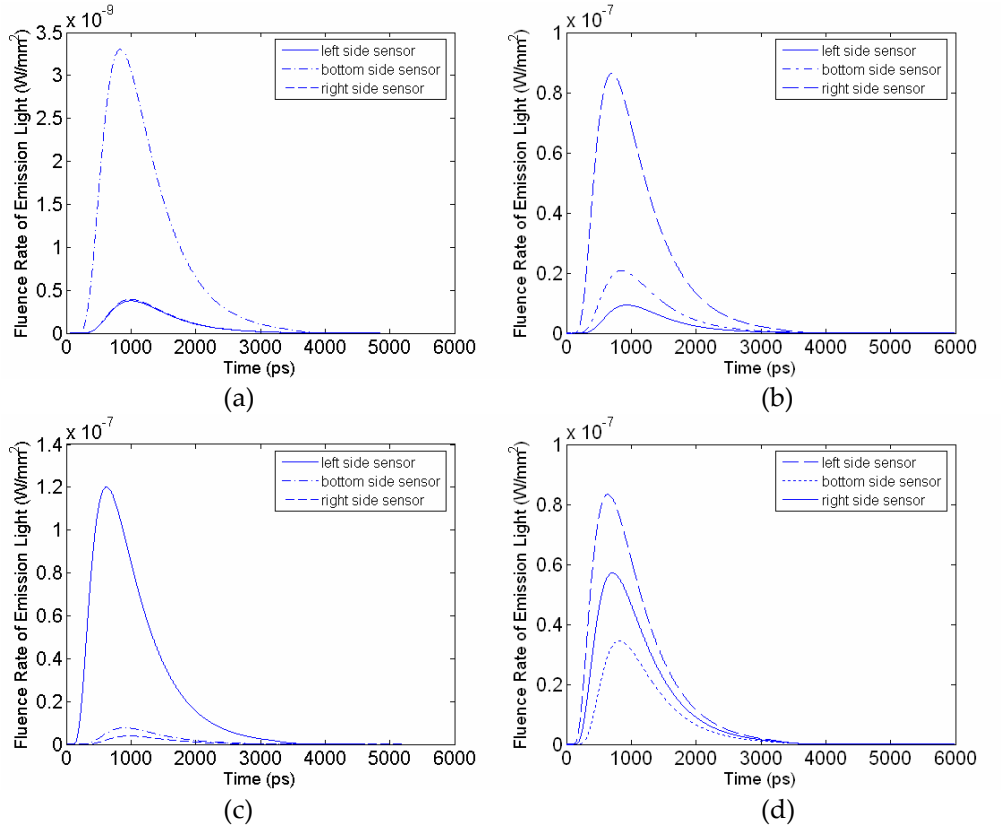

Fig. 2. The intensities of emission light at three main detectors: a) In case of targets 2 and 3 do not exist. b) In case of targets 1 and 3 do not exist. c) In case of targets 1 and 2 do not exist. d) In case of all three targets are embedded inside the model.

We assume there is no fluorophore in the background, therefore the emission lights are found only on the targets that have 1 μM of concentration of the fluorophore, as illustrated in Fig. 3 that shows the distribution of emission light inside the model at 100 and 700ps.

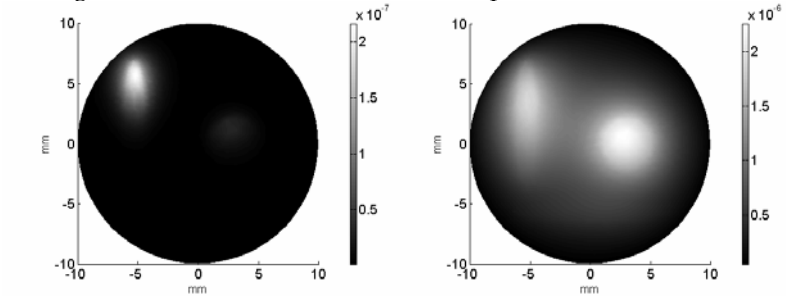

Fig. 3. The emission light distributions of the object in Fig. 1 at 100 and 700 ps (watt mm^{-2}).

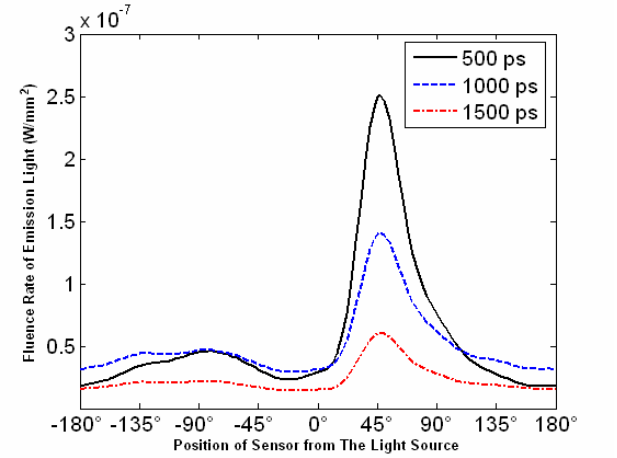

Fig 4. Emission light distribution of object 1 on the boundary at 500, 1000 and 1500 ps (top light)

We have recorded the fluence rate of the emission lights on the boundary at 500, 1000 and 1500 ps. The result is shown in Fig. 4. The distribution of emission light intensity at 1000 ps is higher than the intensity at 500 ps on the area of -180° to 0° with clockwise rotation. Otherwise, the maximum value occurs at the area of 45-50° at 500 ps, and then the emission light will gradually spread to other areas afterwards.

4. Conclusions

We have obtained better results of the distribution of the emission light using a simple method, the zero lifetime convolution algorithms. Recently, we are utilizing these results for developing an inversion process algorithm and trying to yield a better result of the molecular image reconstructions.

The next work is to perform some experiments using phantoms and small animals, and then we would like to compare the measurement results with the results of this work. We hope these calculations will help a lot to our experiment development in order to develop a simple and new image reconstruction method with the better results.

5. References

1. D'Andrea, C. *Localization and Quantification of Fluorescent Inclusion Embedded in a Turbid Medium*. Journal of Physics in Medicine and Biology, 2005.
2. Schulz, R, Peter, J, Semmler, W and Bangerth, W. *Independent Modelling of Fluorescence Excitation and Emission with the Finite Element Method*. Biomedical Topical Meeting of Optical Society of America, 2004.
3. Marjono, A, Feng, G and Yamada, Y. *Time-Resolved Fluorescence Diffuse Optical Tomography Utilizing Generalized Pulse-Spectrum Technique*. 4th World Congress on Industrial Process Tomography (2005).
4. Farrel, T and Patterson, M. *Diffusion Modelling of Fluorescence in Tissue* in Handbook of Biomedical Fluorescence. Marcel Dekker, Inc, 2003.
5. Hillman, E. *Experimental and Theoretical Investigations of Near-Infrared Tomographic Imaging Methods and Clinical Applications*. University College London, 2002.
6. Redmond, R. *Introduction to Fluorescence and Photopysics* in Handbook of Biomedical Fluorescence. Marcel Dekker, Inc, 2003.
7. Kleinschmidt, J. *Spectroscopic Methods in Biochemistry Principles and Applications*. 2000.
8. Boas, D. *Imaging the Body with Diffuse Optical Tomography*. IEEE Signal Processing Magazine, 2001.
9. Marcu, L, Grundfest, W and Fishbein, M. *Time-Resolved Laser-Induced Fluorescence Spectroscopy for Staging Atherosclerotic Lesions* in Handbook of Biomedical Fluorescence. Marcel Dekker, Inc, 2003.
10. Yamada, Y. *Light-Tissue Interaction and Optical Imaging in Biomedicine*. Begell House, Inc, 1995.